Temperature dependence of near-infrared spectra of whole blood

Paul Martinsen
The Food and Horticulture Research Institute
    of New Zealand
Hamilton, New Zealand 3240
E-mail: pmartinsen@hortresearch.co.nz

Jean-Luc Charlier
Auckland City Hospital
Green Lane Perfusion
2 Park Road
Grafton, Auckland 1010
New Zealand

Tim Willcox
Guy Warman
The University of Auckland
Department of Anaesthesiology
Faculty of Medical and Health Sciences
Auckland, New Zealand 1142

Andrew McGlone
The Food and Horticulture Research Institute
    of New Zealand
Hamilton, New Zealand 3240

Rainer Künnemeyer
The University of Waikato
Hamilton, New Zealand 3240

Abstract. The temperature dependence (30 to 40°C) of near-infrared spectra (500 to 1100 nm) of whole human blood, including red blood cells with intact physiological function, is investigated. Previous studies have focused on hemoglobin solutions, but the operation of red blood cells is critically dependent on intact cell membranes to perform normal oxygen transport and other physiological functions. Thus measurements of whole blood are more directly related to changes that occur *in vivo*. In addition to the response of hemoglobin to temperature in the spectra, a temperature response from water in the plasma is also detected. The temperature response of the water absorption at 960 nm is approximately ten times smaller than the temperature response of the oxyhemoglobin component in the blood at 610 nm. However, it is the most significant temperature effect between 800 and 1000 nm. This work will aid the precision and understanding of full spectrum near-infrared measurements on blood. © *2008 Society of Photo-Optical Instrumentation Engineers.* [DOI: 10.1117/1.2943191]

1 Introduction

Nature has provided a window in the near-infrared portion of the electromagnetic spectrum for probing the chemistry of biological samples with light. The near-infrared window, commonly 700 nm to 2.5 μm, is delimited by strong absorbance of hemoglobin and skin pigments at the low end, and by water absorption at the high end.[1] An interesting subset of this range is the Herschel region, which starts at 700 nm and ends at 1100 nm and is the portion accessible by low-cost, silicon semiconductor-based sensors.

One of the most successful applications of near-infrared spectroscopy is *in-vitro* and *in-vivo* measurement of blood oxygen saturation and hemoglobin concentration.[2–4] Consequently, the absorption of oxy- and deoxyhemoglobin has been well studied.[5–9] The impact of temperature on these measurements has received less attention. Refsum and Sveinsson reported a temperature effect on the optical density of hemolyzed blood at 576 and 560 nm in 1956.[10] Refsum expanded on this with measurements of optical density on heparinized venous blood between 3 and 37°C at 576, 560, and

506 nm.[11] The first multispectral results, from 360 to 1010 nm, were reported by San Biagio et al. and showed the absorbance of oxy- and deoxyhemoglobin at 4°C and approximately 24°C in phosphate buffer.[12] They took care to subtract the effect of the water absorption band at 980 nm from their measurements and found that the near-infrared and visible absorption bands of hemoglobin were influenced by temperature. Chuknyiski, Alston, and Rifkind explored the hemoglobin subunits responsible for the temperature dependence in the 380- to 460-nm region[13] in 1985. In 1986, Cordone et al. reported measurements of a hemoglobin-water-glycerol solution from −250 to 27°C.[14] They found the absorption bands of hemoglobin become narrower and shift in wavelength as temperature is decreased. In 1992, Steinke and Shepherd reported optical absorbance spectra of oxy-, carboxy-, and deoxyhemoglobin at wavelengths from 479 to 651 nm and three temperatures: 20, 30, and 40°C. They investigated the error temperature could introduce in a CO-oximeter.[15] In 1997, Sfareni et al. reported temperature-dependent changes of hemoglobin derivatives from 20 to 40°C for the near-infrared region (700 to 1100 nm).[16] Hemoglobin was obtained from lyzed

Address all correspondence to Paul Martinsen, The Food and Horticultural Research Institute of New Zealand, East Street-Hamilton, na 3240 New Zealand; Tel: 64-7-858-4768; Fax: 64-7-585-4705; E-mail: pmartinsen@hortresearch.co.nz
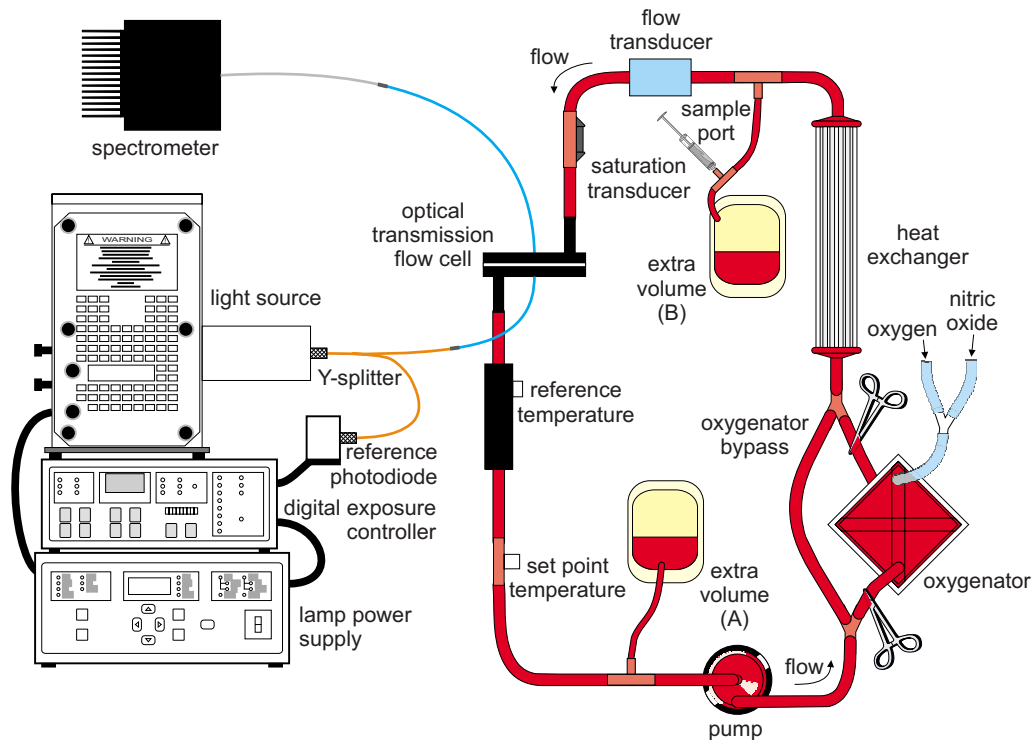
Fig. 1 Schematic illustration of the experimental setup for near-infrared measurement of whole blood.

human blood cells and the effect measured in a phosphate buffer.

All of these earlier studies used hemoglobin solutions. But the operation of red blood cells is critically dependent on the intact cell membrane to perform normal oxygen transport and other physiological functions. In this study, we have made near-infrared optical measurements on whole blood so that the results are more directly related to changes that occur *in vivo*. Our measurements covered temperatures between 30 and 40°C, typical of the range found throughout the human body. The results from these measurements will aid in the understanding and precision of clinical near-infrared measurements on blood. In particular, we see benefits for analysis using full spectrum measurements of blood, such as absolute quantification of oxygen saturation,[17] venous oxyhemoglobin measurements,[18] and measurement of blood pH.[19]

2 Method

The near-infrared optical transmission of fresh (2-day-old) human blood was measured at six different temperatures between 30 and 40°C for each of three different oxygen saturations (80, 90, and 100%). A replicate set of measurements was obtained (next day) using a new sample of blood. The equipment used in the experiment is illustrated in Fig. 1. The measurement order was randomized (separately) for temperature (36, 32, 40, 34, 30, and 38°C) and oxygen saturation (80, 100, and 90%) to reduce temporal correlation.

The optical density was measured in a transmission configuration using a custom-designed flow cell with a physical path length of about 4 mm (Fig. 2). The sample was illuminated using a 50-W halogen lamp mounted in an Oriel lamp housing. Source intensity was stabilized using a Spectra-Physics digital exposure control and Oriel radiometric power supply (Table 1). The transmitted light was measured using a Zeiss MMS-1 spectrometer. The spectrometer and analogue-to-digital (ADC) electronics were kept at constant temperature (~15°C) in a temperature-controlled housing. The light source and spectrometer were connected to the flow cell using 600-μm optical fibers. The source intensity was measured using an integrating sphere (3P-GPS-033-SL, LabSphere®, North Sutton, New Hampshire) in place of the flow cell. Transmittance was calculated as the ratio of blood spectra to the integrating sphere measurement, scaled by 10^{-4} (this scale factor models the attenuation by the integrating sphere).

Blood temperature was monitored using a bead thermistor positioned in the center of the flow a short distance (less than 10 cm) downstream from the optical flow cell. The thermistor resistance was measured using a Keithly multimeter (Keithly, Cleveland, Ohio), then converted to temperature using a prior calibration of the thermistor against a reference thermometer (Hart Scientific 5612, American Fork, Utah). Precision was better than 0.1°C. A LabView™ (National Instruments, Austin, Texas) program automatically recorded both the spectra and blood temperature.

Fresh human whole blood was sourced from the local blood bank and refrigerated during transportation to the test site. The whole blood obtained was of insufficient volume for transfusion and would be discarded ordinarily. Four bags of blood were obtained: two O+ (628 and 550 mL) and one each of A+ (473 mL) and AB+ (642 mL). All were from different donors. Two sets of replicate measurements were obtained across two days. The first with the O+ blood, and the second with the A+ and AB+ blood to make up sufficient volume for the circuit. In each case, the samples were mixed
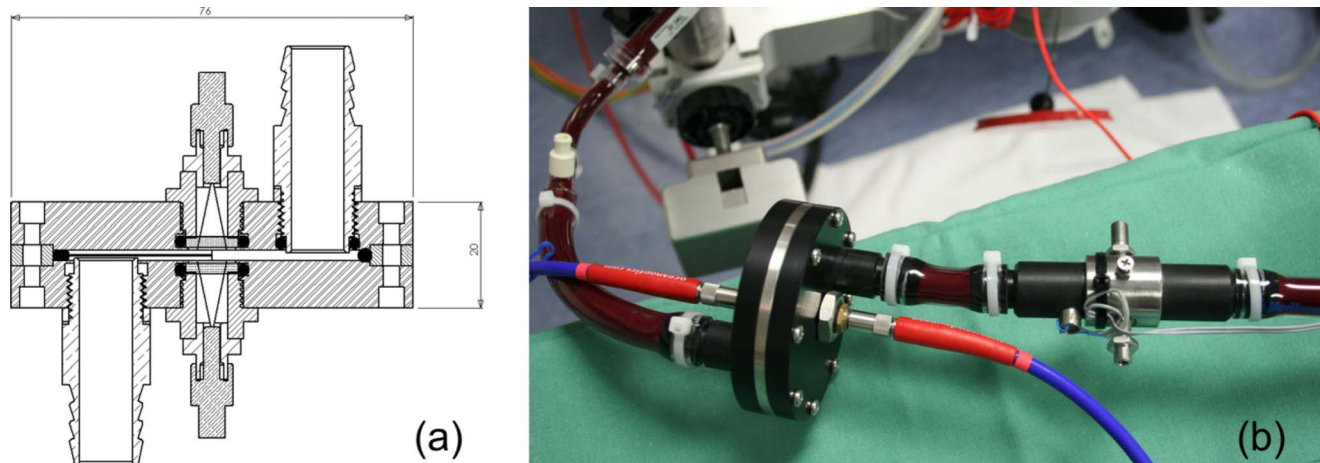
Fig. 2 (a) Cross section of optical flow cell, (b) and photograph of optical flow cell (foreground, left), and temperature measurement flow cell (foreground, right). The source fiber comes in on the left in the photograph.

thoroughly. Ethics approval to use discarded human blood was obtained from the Ministry of Health Northern Regional Ethics Committee (approval number NTY/07/35/EXP).

A circuit constructed from standard components used during cardiopulmonary bypass (Fig. 1) controlled blood flow, oxygen saturation, and temperature of the blood passing through the optical transmission flow cell. Approximately 750 mL of blood was circulated at 2 L/min by a centrifugal pump past an oxygenator, heat exchanger, flow transducer, saturation transducer, the optical flow cell, and temperature sensors. The circuit included a bypass loop around the oxygenator. Details for the components used in the circuit are listed in Table 1. The circuit was initially primed with Plasmalyte® 148 (Baxter Healthcare Pty Limited, New South Wales, Australia). The blood was added to the circuit, replacing the Plasmalyte®. Blood additional to the circuit volume was stored in infusion bag A (Fig. 1). Blood volume withdrawn for sampling was automatically replaced from bag A, maintaining a constant volume in the circuit throughout the experiment.

The membrane oxygenator was included in the circuit only when altering the oxygen saturation of the blood. The saturation of the blood was altered by ventilating the oxygenator with a combination of oxygen and nitric oxide gases. The oxygen saturation was monitored using the Biotrend saturation transducer and the light transmitted by the optical flow cell (which had a faster response than the saturation monitor). Once the target saturation was achieved, the oxygenator was bypassed (by selectively clamping the tubing) to maintain constant oxygen saturation in the circuit. The oxygen saturation was confirmed by blood gas analysis of a 1-mL sample drawn from the sample port (Fig. 1).

Subsamples (4 mL) were also taken at regular intervals to measure free-plasma hemoglobin. Blood gas analysis (Radiometer® ABL800Flex, Brønshøj, Denmark) of these samples was used for measurement of saturation and hematocrit. The hospital's (Auckland City Hospital, New Zealand) regular diagnostic service was used for measurement of free-plasma hemoglobin. As samples were taken, replacement blood automatically added from infusion bag A (Fig. 1) introduced a

Table 1 Details of components used in the circuit for near-infrared measurement of whole blood.

Component	Manufacturer
Jostra Quadrox D centrifugal pump with flow probe	Maquet Cardiopulmonary (Hirrlingen, Germany)
Biotrend saturation transducer	Medtronic (Minneapolis, MN, USA)
TX 40P flow transducer	Medtronic (Minneapolis, MN, USA)
Luer thermistor	Terumo (Ann Arbor, MI, USA
Biotherm heat exchanger	Medtronic (Minneapolis, MN, USA)
Jostra Quadrox D hollow fiber membrane oxygenator, treated with Quadrox Jostra Safeline	Maquet Cardiopulmonary (Hirrlingen, Germany)
Tubing and connectors (class VI 3/8 and 1/4 inch)	Medtronic (Minneapolis, MN, USA)
Infusion bags	Transfer Pack Container, Baxter Healthcare Corporation (Deerfield, IL, USA)
Zeiss MMS-1 spectrometer	Carl Zeiss (Jena, Germany)
Oriel light source	Newport (Irvine, CA, USA)
Spectra-Physics exposure control	Newport (Irvine, CA, USA)
Reference temperature sensor	Custom made
Optical flow cell	Custom made

Table 2 Summary of oxygen saturation (sat O_2) and oxygen partial pressure (PO_2) measured throughout the experiment with a blood gas analyzer for replicate 1 (shaded) and replicate 2. Results are reported in the sequence measured.

T [°C]	80% Sat O_2 [%]		PO_2 [kPa]		100% Sat O_2 [%]		PO_2 [kPa]		90% Sat O_2 [kPa]		PO_2 [kPa]	
36	84.9	78.1	6.36	4.79	99.3	99.6	75.2	72.2	93.3	91.4	10.5	7.77
32		79.0		4.96					93.6		10.6	
40	81.3	79.6	5.66	5.11		99.4		55.4	93.5	91.5	10.8	8.59
34	82.9	79.6	6.46	5.14					93.2		10.7	
30		82.3		5.57					93.1	91.0	10.6	8.27
38	82.6	83.3	6.51	5.64	99.1	99.4	62.0	51.8	92.6	91.3	10.4	8.07

small but measurable change (less than 5%) in the oxygen saturation of the circuit volume.

3 Results

The blood chemistry measurements of the subsamples are reported in Table 2. At 80% nominal saturation, there was a small increase in oxygen saturation with each measurement in the second replicate. This occurred when the oxygen saturation of blood replacing the subsample volume from the reservoir was different from the oxygen saturation in the circuit blood. Hematocrit remained constant throughout the experiment at $30.4 \pm 0.3\%$ and $27.5 \pm 0.9\%$ for the first and second replicate, respectively. (Errors are reported as two standard deviations: a 95% confidence interval.) This is below the normal physiological range of 40 to 54% (male) and 38 to 46% (female), but selection was limited. The lower hematocrit resulted in a scattering coefficient lower than for blood from the "normal" range.

The amount of free hemoglobin in the blood plasma was measured regularly throughout the experiment as an indication of hemolysis. For the first replicate, median plasma hemoglobin was 130 mg/L (110 to 230 mg/L). For the second replicate, median plasma hemoglobin was 320 mg/L (190 to 460 mg/L). There was no clear trend to suggest damage during the experiment. Together, these values suggest only minimal hemolysis of the blood cells so the optical measurement should not be unduly influenced by free hemoglobin in the blood plasma.

The optical transmission spectra for the two samples are plotted in Fig. 3. The separation into three distinct groups, by nominal oxygen saturation, around 700 nm is caused by the large difference in absorption for oxy- and deoxyhemoglobin.[16] The variation within each group is due to temperature. Below 600 nm, the absorption coefficient for oxy- and deoxyhemoglobin increases rapidly so the blood in this region transmits almost no light. As oxygen saturation decreased, the 760-nm absorption peak in deoxyhemoglobin became apparent. The second derivative spectrum (Fig. 4) shows more detail beyond 800 nm, revealing the 840- and 970-nm water absorption bands. These absorptions are probably due to the water that makes up the bulk of the blood plasma. In the second derivative, the 760-nm deoxyhemoglobin peak clearly increased as expected when the oxygen saturation decreased, demonstrating that the blood reached full saturation for the 100% measurement.
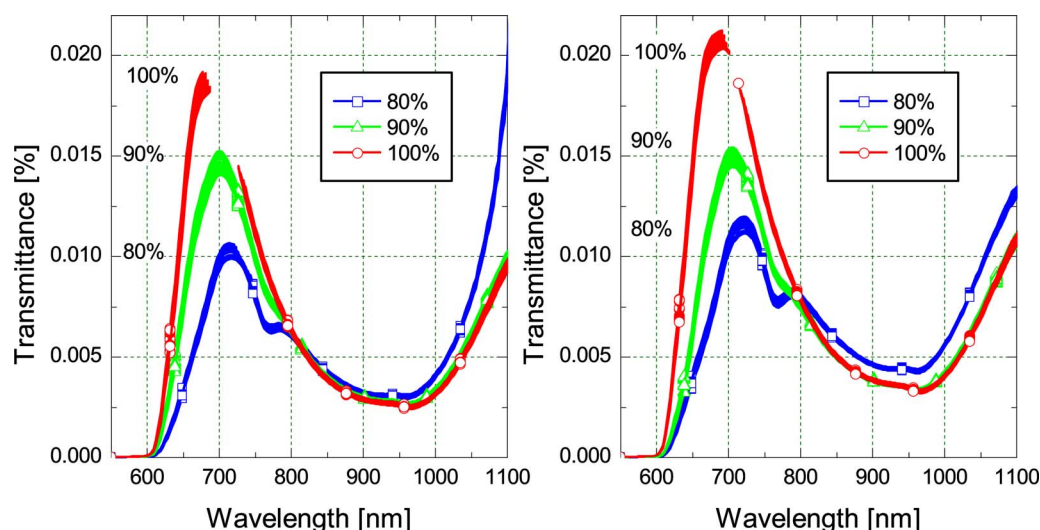

Fig. 3 Near-infrared transmission spectra are plotted for the first (left) and second (right) replicates of the whole blood samples. There is clear separation between the three nominal oxygen saturation groups (labeled). Missing data around 700 nm are due to detector overloading.
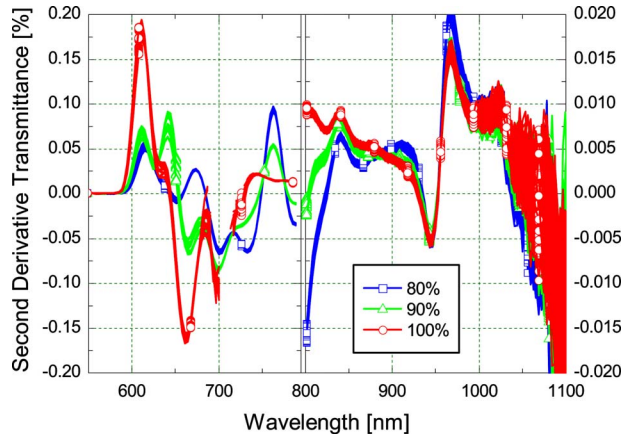
Fig. 4 The second derivative of the near-infrared transmission spectra for the second replicate of whole blood. Note the scale is magnified by ten times to the right of 800 nm for clarity.

4 Discussion

Resolving transmission into an absorption coefficient is difficult for scattering samples, such as whole blood, because the optical path length is not known and is generally much larger than the physical path length. However, it is possible to roughly estimate the optical path length from these measurements using Beer's law. For this we have assumed that the absorption coefficient of blood is dominated by that of water and oxyhemoglobin (at 100% oxygen saturation).[20] The hemoglobin concentration for the two replicates is about 100 g/L. For the transmission observed, this implies a mean optical path length between about 2.5 cm at 970 nm (the strongest water absorption band in our data, though oxyhemoglobin is still the stronger absorber), and about 9 cm at

700 nm. Around 700 nm, scattering dominates; the optical path length is more than 20 times the physical path length. At 970 nm, in contrast, absorption has a larger effect, with the optical path only about six times the physical path length.

More generally, optical density (the negative natural logarithm of transmittance) incorporates the absorption coefficient in a scattering sample. For a nonscattering transmission measurement, dividing the negative logarithm of transmittance by the path length yields the absorption coefficient. In a scattering solution, the optical path length depends on wavelength and scatter concentration, as well as the physical path length between source and detector, so the absorbance cannot be measured by a simple transmission experiment. However, if scatter concentration and absorption do not vary much (as here, for constant oxygen saturation), small changes in absorption produce approximately linear changes in optical density. The three oxygen saturation states were treated separately, so that the large changes in absorption with oxygen saturation did not dominate the relationship.

The temperature coefficient of optical density measurements is plotted in Fig. 5. The temperature coefficient is the slope of a least-squares regression line fitted to temperature versus optical density. For comparison, the absorption temperature coefficient for pure oxyhemoglobin and deoxyhemoglobin,[16] and water[20] are also plotted.

Several features of the data stand out. The temperature coefficients for replicate one are larger than for replicate two. This is probably related to the difference in hematocrit between the two samples. The change in optical density with temperature will act over a longer path length due to more scattering with the higher hematocrit.

The measurements are dominated by large temperature sensitivity below 650 nm that falls sharply at 600 nm. A positive temperature coefficient for hemoglobin in phosphate
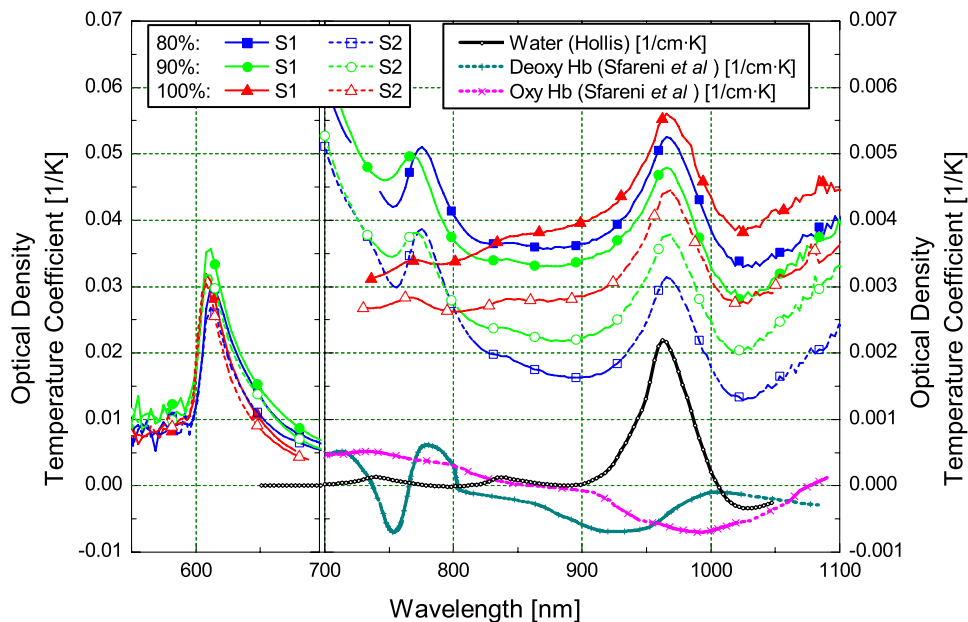

Fig. 5 The temperature coefficient for optical density for each whole blood sample at the three different levels of oxygen saturation is plotted along with the temperature coefficient for the main constituents of blood: water,[20] oxyhemoglobin,[16] and deoxyhemoglobin.[16] The hemoglobin and water absorption have been scaled to their approximate molar concentration in whole blood, 30% hematocrit. Note the change in vertical scale at 700 nm.

buffer down to 565 nm has been reported.[12] However, very little light is transmitted at the low end of this range in our measurements, suggesting we are seeing only the tail of this effect. The main effect is lost in the instrument noise.

The water absorption temperature coefficient around 960 nm is prominent at all oxygen saturations. It is also the likely cause of the subtle bump visible at 840 nm. The origin of the small bump on the 100% oxygen saturation at 760-nm data is less clear. It could be the 740-nm water temperature coefficient peak shifted by the sloping optical density (Fig. 3) but more data are needed to substantiate this.

It is clear then that water makes an important contribution to the temperature coefficient of whole blood in the near-infrared portion of the optical spectrum, particularly between 900 and 1000 nm.

The deoxyhemoglobin temperature coefficient is most apparent in the optical density of whole blood between 750 and 800 nm. As oxygen saturation drops from 100 to 80 and 90%, a wobble appears in the temperature coefficient of whole blood around 770 nm, as Sfareni et al. found for deoxyhemoglobin.[16] The deoxyhemoglobin peak seems disproportionately large compared to the water peak at 960 nm. We believe this is caused by the difference in path length at the two wavelengths.

Also apparent in the data is a general positive temperature effect of 0.003 to 0.004/K that is largely independent of wavelength. With only two replicates, it is difficult to identify the cause of this. A 12- to 16-μm increase in path length might explain it; though this is 100 times greater than can be expected from thermal expansion of the aluminium ring separating the source and detector.[21] The effect is also larger than can be explained by a change in the density of the blood with temperature (approximately 3.8×10^{-4}/K at 37°C[22]). One possibility is flexure of the flow cell, which is constructed from an acetal plastic. Additional work is planned to resolve this question.

Finally, there is a general decrease in the temperature coefficient around 960 nm as oxygen saturation decreases, mirrored by an increase below 800 nm. We suspect two factors contributing to this: path length changing with oxygen saturation and hemoglobin's affinity for oxygen changing with temperature and oxygen saturation.[23]

In a scattering medium, the mean path length traveled between the source and detector depends on both the scattering and absorption coefficients. Typically, as absorption gets smaller, light is scattered through a longer path before being absorbed. For example, when the absorption coefficient of whole blood at 900 nm decreases as the oxygen saturation decreases (shifting the balance between oxy- and deoxyhemoglobin absorbers), the mean path length between the source and detector will increase. Optical density does not separate absorption and path length. The increased path length can increase the optical density and its temperature coefficient. Monte Carlo simulation of photon transport in the flow cell could be used to quantify this effect. Nonetheless, an increasing path length, which would increase the optical density temperature coefficient with oxygen saturation, is contrary to the result in Fig. 5. Again, with only two replicates it is difficult to be conclusive; however, the path length effect may be small or countered by some other effect.

The change in hemoglobin oxygen affinity with temperature would normally cause a change in oxygen saturation: as temperature increases, the oxygen saturation would decrease. The absorption coefficients of oxy- and deoxyhemoglobin are dramatically different, so this shift in oxygen saturation changes the optical density and contributes to the temperature coefficient. A decrease in oxygen saturation increases the absorption coefficient of blood below 800 nm and decreases it above 800 nm. This affects the optical density similarly and matches the result observed in the optical density temperature coefficient.

In our experimental system, there is very little oxygen available to shift the oxygen saturation when temperature changes, only that dissolved in the plasma. We made rough calculations of the optical density change expected from changes in hemoglobin affinity when a surplus of oxygen is available using the mean optical density we measured at 80, 90, and 100%. From this, we suspect the optical density temperature coefficient is 2 to 3 times smaller at 90% and 5 to 7 times smaller at 80% than if more oxygen was available to shift oxygen saturation as hemoglobin affinity changed. Like our experimental setup, the mammalian arterial system lacks a ready supply of oxygen; gas exchange principally occurs in the lungs and capillary bed. So we believe the results reported here will reflect the behavior of arterial blood, but not blood in the lungs or capillaries.

This simple experiment to document the near-infrared temperature coefficient of whole blood has revealed several interesting aspects. More work is planned to explore them further.

5 Conclusion

The effect of temperature on near-infrared transmission spectra of whole human blood, including whole red blood cells with intact physiological function, at three levels of oxygen saturation is measured. As expected, the spectra are dominated by hemoglobin absorption, particularly below 700 nm. At 960 nm, an absorption band is detected and is probably due to absorption by water in the plasma. An optical density temperature coefficient is calculated for each nominal oxygen saturation. Features in the temperature coefficient spectra closely match those of the constituents: oxyhemoglobin, deoxyhemoglobin, and water. The contribution of water to the absorption and temperature coefficient spectra is not apparent in previously reported measurements of hemoglobin using lyzed blood cells. Although the effects are quite small, they may become important when measuring whole blood, particularly in situations involving extreme temperatures, such as during cardiopulmonary bypass. From 900 to 1050 nm, water absorption makes the largest contribution to the temperature coefficient of blood. The temperature response of the water absorption at 960 nm is approximately ten times smaller than the temperature response of the oxyhemoglobin component in the blood at 610 nm. In the method used here, a surplus of oxygen was not available as temperature changed. If surplus oxygen is available, we suspect a larger effect from changes in hemoglobin affinity would be observed in the temperature coefficient. Additional work is planned to explore this.

References

1. V. V. Tuchin, "Light-tissue interactions," in *Biomedical Photonics Handbook*, T. Vo-Dinh, Ed., CRC Press, Oak Ridge, TN (2003).
2. R. N. Pittman, "In vivo photometric analysis of haemoglobin," *Ann. Biomed. Eng.* **14**, 119–137 (1986).
3. G. A. Millikan, "The oximeter, an instrument for measuring continuously the oxygen saturation of arterial blood in man," *Rev. Sci. Instrum.* **13**, 434–444 (1942).
4. N. V. Iftimia, D. X. Hammer, C. E. Bigelow, D. I. Rose, T. Ustun, A. A. Ferrante, V. Danthu, and R. D. Ferguson, "Toward non-invasive measurement of blood hematocrit using spectral domain low coherence interferometry and retinal tracking," *Opt. Express* **14**(8), 3377–3388 (2006).
5. M. Friebel and M. Meinke, "Determination of the complex refractive index of highly concentrated hemoglobin solutions using transmittance and reflectance measurements," *J. Biomed. Opt.* **10**(6), 064019 (2005).
6. A. Roggan, M. Friebel, K. Dörschel, A. Hahn, and G. Müller, "Optical properties of circulating human blood in the wavelength range 400–2500 nm," *J. Biomed. Opt.* **4**(1), 36–46 (1999).
7. M. L. Adams and T. M. Schuster, "Phosphate-dependent spectroscopic changes in liganded haemoglobin," *Biochem. Biophys. Res. Commun.* **58**, 525–531 (1974).
8. F. C. Knowles, M. J. McDonald, and Q. M. Gibson, "The Ørigin of the Adams-Schuster difference spectrum of oxyhemoglobin," *Biochem. Biophys. Res. Commun.* **66**, 556–563 (1975).
9. B. L. Horecker, "The absorption spectra of haemoglobin and its derivatives in the visible and near infra-red regions," *J. Biol. Chem.* **148**(1), 173–183 (1943).
10. H. E. Refsum and S. L. Sveinsson, "Spectrophotometric determination of haemoglobin oxygen saturation in hemolyzed whole blood," *Scand. J. Clin. Lab. Invest.* **8**, 67 (1956).
11. H. E. Refsum, "Influence of hemolysis and temperature on the spectrophotometric determination of haemoglobin oxygen saturation in hemolyzed whole blood," *Scand. J. Clin. Lab. Invest.* **9**, 85–88 (1957).
12. P. L. San Biagio, E. Vitrano, A. Cupane, F. Madonia, and M. Palma, "Temperature induced difference spectra of oxy and deoxy hemoglobin in the near IR, visible and soret regions," *Biochem. Biophys. Res. Commun.* **77**(4), 1158–1165 (1977).
13. P. Chuknyiski, K. Alston, and J. Rifkind, "Temperature dependent spectral changes of iron and nickel hemoglobins and their derivatives," *Biochem. Biophys. Res. Commun.* **128**(2), 721–727 (1985).
14. L. Cordone, A. Cupane, M. Leone, and E. Vitrano, "Optical absorption spectra of deoxy- and oxyhemoglobin in the temperature range 300–20 K," *Biophys. Chem.* **24**, 259–275 (1986).
15. J. M. Steinke and A. P. Shepherd, "Effects of temperature on optical absorbance spectra of oxy-, carboxy- and deoxyhemoglobin," *Clin. Chem.* **38**(7), 1360–1364 (1992).
16. R. Sfareni, A. Boffi, V. Quaresima, and M. Ferrari, "Near infrared absorption spectra of human deoxy- and oxyhaemoglobin in the temperature range 20–40°C," *Biochim. Biophys. Acta* **1340**(2), 165–169 (1997).
17. J. S. Matcher and C. E. Cooper, "Absolute quantification of deoxyhaemoglobin concentration in tissue near infrared spectroscopy," *Phys. Med. Biol.* **39**, 1295–1312 (1995).
18. C. W. Yoxall and A. M. Weindling, "Measurement of venous oxyhaemoglobin saturation in the adult human forearm by near infrared spectroscopy with venous occlusion," *Med. Biol. Eng. Comput.* **35**, 331–336 (1997).
19. N. A. Rosen, W. E. Charash, and E. F. Hirsch, "Near-infrared spectrometric determination of blood pH," *J. Surg. Res.* **106**(2), 282–286 (2002).
20. V. S. Hollis, "Non-invasive monitoring of brain tissue by near-infrared spectroscopy," PhD Thesis, p. 122, Univ. College London, (2002).
21. "Thermal and physical properties of pure metals," in *CRC Handbook of Chemistry and Physics*, 79th ed., D. R. Lide, Ed., pp. 12–191, (CRC Press, Boca Raton, (1986).
22. T. Kenner, "The measurement of blood density and its meaning," *Basic Res. Cardiol.* **84**, 111–124 (1989).
23. M. G. Scott, V. A. LeGrys, and J. S. Klutts, "Electrolytes and blood gases," in *Clinical Chemistry and Molecular Diagnostics*, C. A. Burtis, E. R. Ashwood, and D. E. Bruns, Eds., Elsevier Saunders, St Louis, MO (2006).